

# Double phase conjugate mirror using $\text{Sn}_2\text{P}_2\text{S}_6$ for injection locking of a laser diode bar

Tobias Bach, Mark Fretz, Mojca Jazbinšek, and Peter Günter

Nonlinear Optics Laboratory, ETH Zurich, CH-8093 Zurich, Switzerland

[nlo@phys.ethz.ch](mailto:nlo@phys.ethz.ch)

**Abstract:** We demonstrate double phase-conjugation in pure and Te-doped  $\text{Sn}_2\text{P}_2\text{S}_6$ , a semiconducting ferroelectric material, at the wavelength of 685 nm. We observe a phase conjugate reflectivity of more than 800 % at an intensity ratio of the pump beams of 44 for Te-doped  $\text{Sn}_2\text{P}_2\text{S}_6$ . Using a laser diode bar emitting at 685 nm, we demonstrate double phase conjugation of three independent emitters of the laser diode bar with a single mode master laser. By adjusting the center wavelength of the master laser to the center wavelength of an emitter with an accuracy of less than 0.1 nm, locking of any emitter of the laser diode bar is demonstrated. We improve the spectral width of the emitter from 0.5 nm to below  $2.5 \cdot 10^{-4}$  nm.

© 2008 Optical Society of America

**OCIS codes:** (160.5320) Photorefractive materials; (190.5040) Phase conjugation; (140.3520) Lasers, injection-locked.

---

## References and links

1. S. Weiss, S. Sternklar, and B. Fischer, "Double phase-conjugate mirror – Analysis, demonstration, and applications," *Opt. Lett.* **12**, 114–116 (1987).
2. D. Wang, Z. Zhang, Y. Zhu, S. Zhang, and P. Ye, "Observations on the coupling channel of two mutually incoherent beams without internal reflections in  $\text{BaTiO}_3$ ," *Opt. Commun.* **73**, 495–500 (1989).
3. M. D. Ewbank, "Mechanism for photorefractive phase conjugation using incoherent beams," *Opt. Lett.* **13**, 47–49 (1988).
4. R. W. Eason and A. M. C. Smout, "Bistability and noncommutative behavior of multiple-beam self-pulsing and self-pumping in  $\text{BaTiO}_3$ ," *Opt. Lett.* **12**, 51–53 (1987).
5. M. D. Ewbank, R. A. Vazquez, R. R. Neurgaonkar, and J. Feinberg, "Mutually pumped phase conjugation in photorefractive strontium barium niobate: theory and experiment," *J. Opt. Soc. Am. B* **7**, 2306–2316 (1990).
6. C. Medrano, M. Zgonik, S. Berents, P. Bernasconi, and P. Günter, "Self-pumped and incoherent phase conjugation in Fe-doped  $\text{KNbO}_3$ ," *J. Opt. Soc. Am. B* **11**, 1718–1726 (1994).
7. M. P. Petrov, S. L. Sochava, and S. I. Stepanov, "Double phase conjugate mirror using a photorefractive  $\text{Bi}_2\text{TiO}_{20}$  crystal," *Opt. Lett.* **14**, 284–286 (1989).
8. K. Shcherbin, "Recent Progress in Semiconductor Photorefractive Crystals," in *Photorefractive Materials and Their Applications II*, P. Günter and J.-P. Hiugnard, eds. (Springer-Verlag, New York, 2007), pp. 391–418.
9. G. W. Ross and R. W. Eason, "Double phase-conjugate mirror with sixfold gain in photorefractive  $\text{BaTiO}_3$  at near-infrared wavelengths," *Opt. Lett.* **18**, 571–573 (1993).
10. R. S. Cudney and M. Kaczmarek, "Optical poling in  $\text{Rh}:\text{BaTiO}_3$ ," in *Trends in Optics and Photonics*, Vol. 62, pp. 485–489 (2001).
11. M. B. Klein, "Photorefractive Properties of  $\text{BaTiO}_3$ ," in *Photorefractive materials and their applications I*, P. Günter and J.-P. Hiugnard, eds. (Springer Verlag, Berlin, 1988), pp. 195–236.
12. P. Yeh, *Introduction to Photorefractive Nonlinear Optics* (John Wiley and Sons, Inc., 1993).
13. M. Cronin-Golomb, B. Fischer, J. O. White, and A. Yariv, "Theory and applications of four-wave mixing in photorefractive media," *IEEE J. Quantum Electron.* **QE-20**, 12–30 (1984).
14. D. Engin, M. Segev, S. Orlov, and A. Yariv, "Double phase conjugation," *J. Opt. Soc. Am. B* **11**, 1708–1717 (1994).

15. N. Wolffer, P. Gravey, J. Y. Moisan, C. Laulan, and J. C. Launay, "Analysis of double phase conjugate mirror interaction in absorbing photorefractive crystals: application to BGO:Cu," *Opt. Commun.* **73**, 351–356 (1989).
16. S. MacCormack, J. Feinberg, and M. H. Garret, "Injection locking a laser-diode array with a phase conjugate beam," *Opt. Lett.* **19**, 120–122 (1994).
17. K. Iida, H. Horiuchi, O. Matoba, T. Omatsu, T. Shimura, and K. Kuroda, "Injection locking of a broad-area diode lasers through a double phase conjugate mirror," *Opt. Commun.* **146**, 6–10 (1998).
18. F. Wang, A. Hermerschmidt, and H. J. Eichler, "High-power narrowed-beandwidth output of a broad-area multiple-stripe diode laser with photorefractive phase-conjugated injection," *Opt. Commun.* **209**, 391–395 (2002).
19. A. A. Grabar, M. Jazbinsek, A. N. Shumelyuk, Y. M. Vysochanskii, G. Montemezzani, and P. Günter, "Photorefractive effects in  $\text{Sn}_2\text{P}_2\text{S}_6$ ," in *Photorefractive Materials and Their Applications II*, P. Günter and J.-P. Huignard, eds. (Springer-Verlag, New York, 2007), pp. 327–362.
20. S. G. Odoulov, A. N. Shumelyuk, U. Hellwig, R. A. Rupp, and A. A. Grabar, "Photorefractive beam coupling in tin hypophosphite in the near infrared," *Opt. Lett.* **21**, 752–754 (1996).
21. M. Jazbinsek, G. Montemezzani, P. Günter, A. A. Grabar, I. M. Stoika, and Y. M. Vysochanskii, "Fast near-infrared self-pumped phase conjugation with photorefractive  $\text{Sn}_2\text{P}_2\text{S}_6$ ," *J. Opt. Soc. Am. B* **20**, 1241–1246 (2003).
22. M. Jazbinšek, D. Haertle, G. Montemezzani, P. Günter, A. A. Grabar, I. M. Stoika, and Y. M. Vysochanskii, "Wavelength dependence of visible and near infrared photorefractive and phase conjugation in  $\text{Sn}_2\text{P}_2\text{S}_6$ ," *J. Opt. Soc. Am. B* **22**, 2459–2467 (2005).
23. R. Mosimann, P. Marty, T. Bach, F. Juvalta, M. Jazbinsek, P. Günter, and A. A. Grabar, "High-speed photorefractive telecommunication wavelength  $1.55\ \mu\text{m}$  in  $\text{Sn}_2\text{P}_2\text{S}_6:\text{Te}$ ," *Opt. Lett.* **32**, 3230–3232 (2007).
24. T. Bach, M. Jazbinsek, P. Günter, A. A. Grabar, I. M. Stoika, and Y. M. Vysochanskii, "Self pumped optical phase conjugation at  $1.06\ \mu\text{m}$  in Te-doped  $\text{Sn}_2\text{P}_2\text{S}_6$ ," *Opt. Express* **13**, 9890–9896 (2005).
25. T. Bach, M. Jazbinsek, G. Montemezzani, P. Günter, A. A. Grabar, and Y. M. Vysochanskii, "Tailoring of infrared photorefractive properties of  $\text{Sn}_2\text{P}_2\text{S}_6$  crystals by Te and Sb doping," *J. Opt. Soc. Am. B* **24**, 1535–1541 (2007).
26. A. A. Grabar, I. V. Kedyk, M. I. Gurzan, I. M. Stoika, A. A. Molnar, and Y. M. Vysochanskii, "Enhanced photorefractive properties of modified  $\text{Sn}_2\text{P}_2\text{S}_6$ ," *Opt. Commun.* **188**, 187–194 (2001).

## 1. Introduction

The photorefractive (PR) double phase-conjugate mirror (DPCM) is based on a four-wave mixing geometry first demonstrated by Weiss et. al [1]. Its capability of coupling two independent (mutually incoherent) laser sources makes it of unique interest for optical applications. DPCM was realized in many different geometries, which can be categorized by the number of internal reflections the beams experience in the crystal: zero reflections (double phase conjugation and modified bridge) [1, 2], one reflection (bird-wing) [3], two reflections (mutually incoherent beam coupling, MIPC) [4] and three reflections (frog-legs) [5]. The mostly implemented material of choice in these configurations is ferroelectric  $\text{BaTiO}_3$ , because it shows the highest phase conjugate reflectivity compared to ferroelectric  $\text{LiNbO}_3$  and  $\text{KNbO}_3$  [6], sillenite-type crystals [7] and semiconductors [8] where DPCM was also investigated. With  $\text{BaTiO}_3$  a maximal double phase conjugate reflectivity of more than 600 % at a wavelength of  $\sim 800\text{nm}$  was measured [9]. However,  $\text{BaTiO}_3$  shows a very slow grating build-up time particularly for infrared wavelengths and in addition suffers from domain formation caused by infrared light [10]. Also the tetragonal-orthorhombic phase transition is very close to room temperature at  $\sim 9^\circ\text{C}$  [11], therefore a new material is preferable for real-life applications using a DPCM.

The performance parameters of a double phase conjugate mirror can be described theoretically by the plane-wave solutions of coupled-wave equations with large coupling (pump depletion) [12–14]. In this model absorption losses are neglected. By considering the absorption, the optical energy is not conserved in the crystal and the coupled-wave equations cannot be integrated directly. Numerical calculations give solutions for the reflectivity of the double phase conjugate mirror with large coupling including absorption losses [15].

A very important application of the double phase-conjugate mirror is spectral laser beam clean-up of semiconductor lasers. Semiconductor lasers exist in various designs. Single mode laser diodes have a good spectral profile but a small output power. To increase the output power

one has to increase the active area in the laser diode leading to a broader spectrum. Broad area diode lasers have a uniform active area where light is emitted. Laser diode arrays are interrupted in the active area to increase the cooling capability of the device, but the emitting areas are still not independent of each other and the output characteristics are similar to a single emitter. Laser diode bars (or stacks) reach the highest output power among semiconductor lasers. Here either laser diode arrays or single independent emitters are placed next to each other in a single device.

To achieve spectral laser beam clean-up, a powerful semiconductor laser of a broad spectrum (slave laser) can be locked with the help of a DPCM to a low power laser of a narrow spectrum (master laser). After locking the slave laser oscillates at the same frequency as the master laser and has similar (improved) spectral properties. This was successfully demonstrated, e.g. by MacCormack et. al, for a laser diode array coupled to a single-mode laser diode [16]. To increase the output power, Iida et al. [17] showed injection locking of a high-power broad-area diode laser to a single-mode master laser and Wang et al. [18] the coupling of a broad-area multiple-stripe diode laser. To our knowledge, spectral laser beam clean-up using a DPCM has not yet been investigated with a laser diode bar.

In this paper we demonstrate for the first time double phase conjugation in tin thiodiphosphate ( $\text{Sn}_2\text{P}_2\text{S}_6$ ) and double phase conjugation of several emitters of a laser diode bar with a single-mode master laser.  $\text{Sn}_2\text{P}_2\text{S}_6$  is a relatively new photorefractive ferroelectric crystal [19] with a very high electro-optic figure of merit  $n^3r = (4800 \pm 300) \text{ pm/V}$  at 633 nm, extremely fast photorefractive response in the red and infrared [20–22] compared to other ferroelectric crystals and is even sensitive at telecommunication wavelength  $1.55 \mu\text{m}$  [23]. Self-pumped optical phase conjugation was demonstrated up to a wavelength of  $1.06 \mu\text{m}$  with Te-doped  $\text{Sn}_2\text{P}_2\text{S}_6$  with the reflectivity of more than 40 % and rise time below 100 ms at  $20 \text{ W/cm}^2$  light intensity [24], which is two orders of magnitude faster compared to Rh-doped  $\text{BaTiO}_3$ . Here we present results of phase conjugate reflectivities of more than 800 % at the wavelength of 685 nm, to our knowledge the highest reported reflectivity for double phase conjugate mirrors. Experimental results of the variation of the intensity ratio of the incoming beams, as well as the variation of the total intensity, are compared with a modified model of the plane wave solutions of coupled wave equations. We also demonstrate the spectral beam clean-up of one emitter of a laser diode bar with a single mode laser diode at 685 nm. Simultaneous phase conjugation of three emitters of the laser diode bar with the seeder laser is demonstrated at 685 nm. By adjusting the wavelength of the seeder laser to the wavelength of one of the three emitters of the laser diode bar with a precision of  $< 0.1 \text{ nm}$ , each emitter can be locked and spectrally cleaned.

## 2. Experiment

In our experimental configurations with double phase conjugated mirrors we used nominally pure or Te-doped  $\text{Sn}_2\text{P}_2\text{S}_6$  crystals as the photorefractive phase-conjugate couplers. Nominally pure crystals are of yellow color and crystals doped with Te are of light brown color due to the shift of the absorption edge in Te-doped crystals [25].

At room temperature  $\text{Sn}_2\text{P}_2\text{S}_6$  has a ferroelectric monoclinic structure with point group symmetry  $m$  [19]. We use a coordinate system with the  $z$ -axis parallel to the crystallographic  $c$ -axis, the  $y$ -axis normal to the mirror plane and the  $x$ -axis (which is close to the axis of the spontaneous polarization) normal to  $y$  and  $z$  [19]. The samples were oriented by X-rays, cut along the  $x$ ,  $y$  and  $z$  axes and polished normal to the  $z$ -axis. Crystals were poled by applying an electric field of about  $500 \text{ V/cm}$  along the  $x$ -axis above the phase transition temperature  $T_c = 337 \text{ K}$  and then slowly cooled down to room temperature with the applied electric field on. The maximal photorefractive gain  $\Gamma$  for nominally pure crystals is  $\Gamma = 7 \text{ cm}^{-1}$  at a wavelength of 633 nm and  $\Gamma = 2.5 \text{ cm}^{-1}$  at 780 nm [22]. The corresponding grating recording times  $\tau$  at an intensity of  $10 \text{ W/cm}^2$  are  $\tau = 5 \text{ ms}$  and  $\tau = 10 \text{ ms}$  at the wavelengths 633 nm and 780 nm, respectively. For

Te-doped  $\text{Sn}_2\text{P}_2\text{S}_6$  these values are:  $\Gamma = 10\text{ cm}^{-1}$  and  $\tau = 0.1\text{ ms}$  at  $633\text{ nm}$  and  $\Gamma = 6\text{ cm}^{-1}$  and  $\tau = 0.2\text{ ms}$  at  $780\text{ nm}$  [25].

### 2.1. Optimized double phase conjugation

To characterize the double phase conjugate mirror we chose a set-up with a Te-doped  $\text{Sn}_2\text{P}_2\text{S}_6$  crystal with dimensions  $x \times y \times z = 10\text{ mm} \times 6\text{ mm} \times 7.44\text{ mm}$  (Fig. 1). As master laser we used a laser diode (wavelength  $\lambda = 685\text{ nm}$ ) stabilized with a diffraction grating (line density of  $2200\text{ mm}^{-1}$ ) as external cavity to achieve single mode operation (Toptica Photonics). The maximal output power was  $57\text{ mW}$  at a driving current of  $132\text{ mA}$ . The laser diode was optically isolated to prevent that the phase conjugated beams disturb the laser. The beam was split by a beam splitter and the two beams entered a Te-doped  $\text{Sn}_2\text{P}_2\text{S}_6$  crystal from the  $z$ -plane in opposite directions, where they overlapped so that a phase conjugate grating was recorded. To reduce the Fresnel losses, the crystal was coated with a  $190\text{ nm}$  thick  $\text{Al}_2\text{O}_3$  layer. The external angles were adjusted to  $\theta_1 = 20^\circ$  and  $\theta_3 = 60^\circ$  with respect to the sample normal and led to single reflection losses at the crystal surfaces of approximately  $R_0 = 6\%$  and  $R_L = 7\%$ , for beams entering the crystal at  $z = 0$  and  $z = L$ , respectively. The angle difference  $\theta_3 - \theta_1 = 40^\circ$  corresponds to the maximum measured two-wave mixing gain  $\Gamma = 10\text{ cm}^{-1}$  at  $\Lambda = 1.0\text{ }\mu\text{m}$  [25]. An additional glass plate was placed into the path of beam  $A_1$  after the beam splitter to be able to measure the phase conjugate (signal) beam 4. The maximal intensities of beam  $A_1$  and beam  $A_3$  at the position of the crystal were  $I_{10} = 0.18\text{ W/cm}^2$  and  $I_{3L} = 0.17\text{ W/cm}^2$ , respectively. To change the intensity ratio  $q = I_{3L}/I_{10}$ , neutral density (ND) filters were placed in the beam path of beam  $A_1$  for higher ratios and in the path of beam  $A_3$  for smaller ratios. To avoid reflection gratings in the crystal a piezoelectric transducer was used to vibrate one mirror in the path of beam  $A_1$ , making the two input beams incoherent. No additional cylindrical lenses were needed to avoid conical diffraction [7], because the beam profile out of the laser diode is of elliptical shape and therefore the profile of beam  $A_1$  and beam  $A_3$  as well.

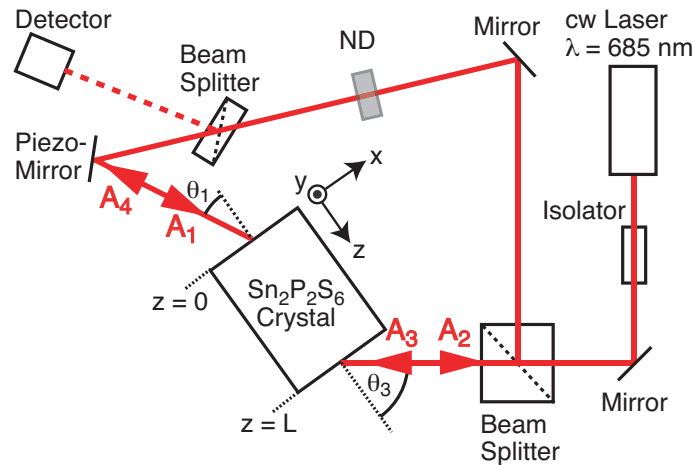


Fig. 1. Experimental set-up for double phase conjugation characterization with a Te-doped  $\text{Sn}_2\text{P}_2\text{S}_6$  crystal at  $685\text{ nm}$ . The phase conjugated beam  $A_4$  is partly reflected by a glass plate and measured by a photodiode. The intensity ratio can be changed by putting filters in the path of beam  $A_1$  or  $A_3$ . The beams are linearly polarized in the plane of incidence.

## 2.2. Double phase conjugation of multiple beams and locking of one emitter

To demonstrate simultaneous phase conjugation of several independent emitters of a laser diode bar with a master laser we used the set-up illustrated in Fig. 2. As the photorefractive material we used a pure (yellow)  $\text{Sn}_2\text{P}_2\text{S}_6$  crystal with dimensions  $x \times y \times z = 8.05 \text{ mm} \times 8.91 \text{ mm} \times 9.72 \text{ mm}$ . The slave laser was a laser diode bar (Coherent, Model B1-69-5C-19-10-A) operating at a constant current and stable temperature at the wavelength of  $686 \pm 2 \text{ nm}$ . It consists of 19 equidistant active areas (emitters) on a width of 1 cm with a fill factor of 50%. The total optical power at maximum driving current of 8 A was 4 W. A cylindrical lens was mounted in front of the laser diode bar to collimate the fast axis. To select any of the emitters (one or several) two moveable blades were placed in front of the laser diode bar. As master laser we used the same single mode laser as in the previous part (Toptica Photonics). By rotating the grating and/or changing the temperature of the laser diode, we could adjust the output wavelength in the range of 683–686 nm.

A cylindrical lens L1 (with focal length  $f_1 = 250 \text{ mm}$ ) was slightly focusing the beam of the slave laser onto the crystal. The cylindrical lenses L2 and L3 ( $f_2 = 60 \text{ mm}$  and  $f_3 = 40 \text{ mm}$ ) were placed in front of the crystal to focus the beams vertically and to prevent conical diffraction in the double phase conjugating process (see e.g. [7]). The angles  $\theta_1$  and  $\theta_2$  could be adjusted to arbitrary values by rotating the  $\text{Sn}_2\text{P}_2\text{S}_6$  crystal and changing the beam path of the slave laser with two mirrors.

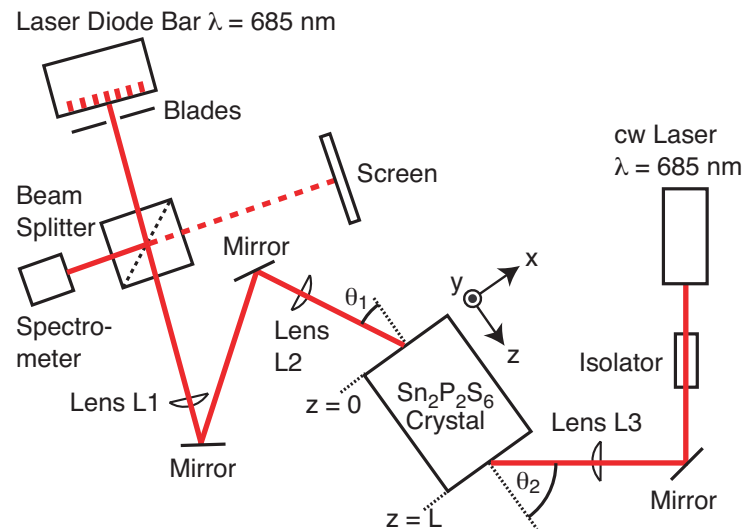


Fig. 2. Experimental set-up for phase conjugate injection locking with laser diodes at around 685 nm and  $\text{Sn}_2\text{P}_2\text{S}_6$  crystal. The laser beams are linearly polarized in the plane of incidence.

## 3. Result and discussion

### 3.1. Phase conjugation for different intensity ratios

Figure 3 shows experimental time evolution of the phase conjugate reflectivity  $R$  after turning on the two beams 1 and 3 at time  $t = 0 \text{ s}$  for a Te-doped  $\text{Sn}_2\text{P}_2\text{S}_6$  crystal. The rise time defined as  $\tau_{90\%} - \tau_{10\%}$  is approximately 7 s for a total intensity of  $I_0 = I_{10} + I_{3L} = 0.15 \text{ W/cm}^2$  in the crystal, considering also the Fresnel losses at the crystal surfaces. By recalculating the rise time to an intensity of  $20 \text{ W/cm}^2$  we get  $\tau_{90\%} - \tau_{10\%} \approx 50 \text{ ms}$ , the same order of magnitude compared

to the rise time of self-pumped phase conjugation at  $1.06\ \mu\text{m}$  in the same Te-doped  $\text{Sn}_2\text{P}_2\text{S}_6$  crystal [24]. We recorded the phase conjugated beam for 450 s to check the long-term stability of the generated signals.

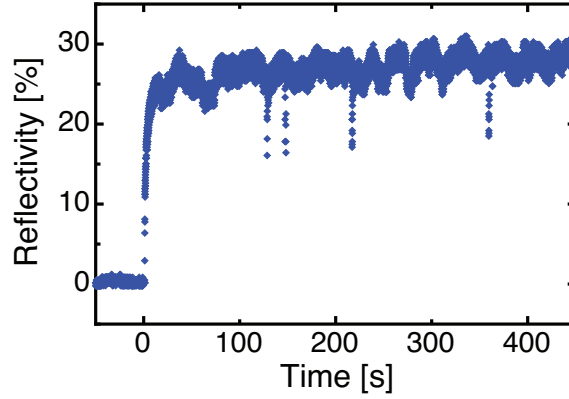


Fig. 3. Long-term measurement of the phase-conjugate reflectivity of beam 4 for an intensity ratio  $q = I_{10}/I_{3L} = 0.9$  of the pump beams. The phase conjugate beam 4 is measured for 450 s to check the stability of the double phase conjugate mirror.

For the theoretical description of our experiment we use the plane-wave description and the coupled wave equations for the case of large coupling (depleted pump) and negligible absorption [12, 13]. The boundary conditions for our double phase conjugate mirror are  $A_2(0) = A_4(L) = 0$ , where  $A_i(z)$  is the electric field amplitude of the  $i$ th wave at position  $z$  along the propagation; we define  $z = 0$  is at the crystal boundary on the side where we measure the phase conjugate reflectivity and  $z = L$  is on the side of the pump beam. The total light intensity is equal to  $I_0 = |A_1|^2 + |A_2|^2 + |A_3|^2 + |A_4|^2 = |A_1(0)|^2 + |A_3(L)|^2 = I_{10} + I_{3L}$  and is independent of  $z$  if absorption is neglected. The four coupled-wave equations can be integrated to obtain the solution in the form [12, 13]

$$s = I_0 \tanh(\kappa L), \quad (1)$$

where

$$s = \sqrt{\sigma^2 + |\rho_0|^2 (I_0 + \sigma)^2}, \quad (2)$$

$$\sigma = I_0 \frac{1 - q}{1 + q}, \quad (3)$$

$$\kappa = \frac{s\Gamma^*}{4I_0}. \quad (4)$$

In Eq. (2),  $|\rho_0|^2$  is the phase-conjugate reflectivity on one side of the crystal (at the position  $z = 0$ ) defined as:

$$|\rho_0|^2 = \left| \frac{A_4(0)}{A_1^*(0)} \right|^2. \quad (5)$$

By inserting Eqs. (2)–(4) into Eq. (1) one obtains the transcendental equation for the reflectivity  $|\rho_0|^2$ , which depends on the coupling constant  $\Gamma L$  and the intensity ratio  $q = I_{3L}/I_{10}$  but not on the total intensity  $I_0$ . The measured reflectivity is equal to  $R = |\rho_0|^2 |t_0|^4$ , where  $t_0$  accounts for the changes in amplitudes and phases of interacting beams after being transmitted through the

sample surface at  $z = 0$ . The single reflection loss at  $z = 0$  in our experiment was  $R_0 = 6\%$ , leading to  $|t_0|^4 = (1 - R_0)^2 \approx 0.88$ .

Figure 4 shows experimental data (points) of the saturated (maximal) phase conjugate reflectivity for different intensity ratios  $q = I_{3L}/I_{10}$ . The highest phase conjugate reflectivity of more than 800% was achieved for an intensity ratio  $q = I_{3L}/I_{10} \approx 44$ . For higher intensity ratios the double phase conjugation breaks down, since we reach the threshold coupling constant ( $\Gamma L$ ), which is a function of the intensity ratio  $q$  [12].

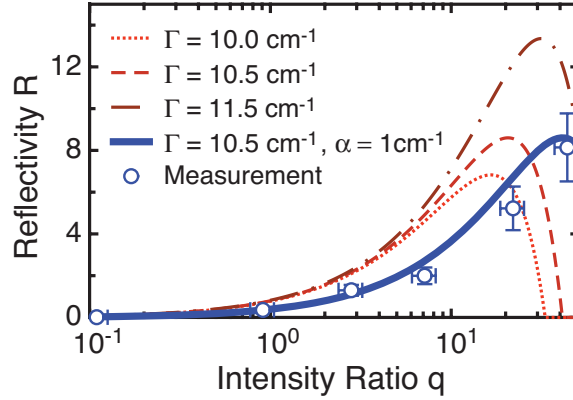


Fig. 4. Saturated phase conjugated reflectivity  $R$  as a function of the intensity ratio  $q = I_{10}/I_{3L}$ . Measured data (points) is compared with calculations. Dotted/dashed curves are based on Eq. (1) for the gain coefficients  $\Gamma = 10\text{cm}^{-1}$ ,  $\Gamma = 10.5\text{cm}^{-1}$  and  $\Gamma = 11.5\text{cm}^{-1}$ . The solid line includes a correction term  $\xi$  for the intensity ratio  $q$  due the absorption loss in the crystal (see Eq. (6)).

Figure 4 also shows the curves calculated using Eq. (1) for varying the gain coefficient within the error from the two-wave mixing experiments:  $\Gamma = 10.0\text{cm}^{-1}$ ,  $\Gamma = 10.5\text{cm}^{-1}$  and  $\Gamma = 11.5\text{cm}^{-1}$ , corresponding to coupling constants of  $\Gamma L = 7.4$ ,  $\Gamma L = 7.8$  and  $\Gamma L = 8.6$ , respectively. The calculation shows best agreement with the measurement for a coupling constant of  $\Gamma L = 7.8$  regarding the absolute value of the measured double phase conjugate reflectivity  $R$ . However, the calculations based on Eq. (1) still have a discrepancy in the intensity ratio  $q$  compared with the measurements. Since in our crystal the absorption constant is  $\alpha \approx 1.0\text{cm}^{-1}$  at the wavelength 685 nm, the absorption is not negligible and therefore the optical energy is not conserved in the crystal and the coupled-wave equations cannot be integrated directly. Numerical calculations for the diffraction efficiency in a double phase conjugate mirror [15], however, have shown that for coupling strength of  $\Gamma L = 7.8$  and for a ratio of  $\Gamma/2\alpha \approx 5$  the discrepancy between considering the absorption and neglecting it is below 10%. Nevertheless, this simplification is not true for the intensity ratio  $q$ . The reduction  $r$  of the intensity over the whole crystal length  $L = 0.744\text{cm}$  is in our  $\text{Sn}_2\text{P}_2\text{S}_6$  crystal  $r = e^{-\alpha L} \approx 0.5$ . Therefore, the intensity ratio at the position  $z = 0$  is  $q_0 = (rI_{3L})/I_{10} \approx 0.5q$  and at the position  $z = L$  is  $q_L = I_{3L}/(rI_{10}) \approx 2q$ . This means that over the propagation length in the crystal from  $z = 0$  to  $z = L$  we get a variation of the intensity ratio from  $0.5q$  to  $2q$ . We consider the part close to  $z = 0$  to be the dominant part in the double phase conjugate process, because the threshold coupling constant  $\Gamma L$  is a function of the intensity ratio  $q$  and increases for increasing  $q$  [12]. Therefore we introduce in Eq. (3) a correction term  $\xi$

$$\sigma = I_0 \frac{1 - q\xi}{1 + q\xi} \quad (6)$$

and in first approximation we choose  $\xi$  so that the intensity ratio  $q$  equals the intensity ratio at

the position  $z = 0$ . This leads to  $\xi = e^{-\alpha L} \approx 0.5$ .

A calculation for the phase conjugate reflectivity  $R$  based on Eq. (1), considering also the correction term  $\xi \approx 0.5$  and for a coupling strength of  $\Gamma L = 7.8$ , is shown in Fig. 4 (solid curve) and is in very good agreement with the measurement.

The solution of the coupled-wave equations for the double phase conjugate mirror does not involve any intensity dependence of the saturated reflectivity on the input beam intensity  $I_0$ . As also observed in a self-pumped ring-cavity phase conjugator, one has to modify the model and take into account the dark conductivity of the crystal [21,24]. The dark conductivity is in competition with the photoconductivity leading to an intensity dependence of the photorefractive gain. Inclusion of the dark conductivity is usually done by introducing an additional parameter  $I_\beta$  called background uniform illumination. To check the validity of our model for the double phase conjugate mirror we measured the phase conjugate reflectivity for reduced input beam intensities for an intensity ratio of  $q = 0.91$ . The results are shown Fig. 5. The saturated reflectivity increases for lower intensities and then saturates for higher intensities. This means that for lower intensities we also have to take into account the background uniform illumination  $I_\beta$  into the model for the double phase conjugate mirror, which will change the parameter  $\kappa$  in Eq. (4) to

$$\kappa = \frac{s\Gamma^*}{4(I_0 + I_\beta)}. \quad (7)$$

The dotted/dashed curves in Fig. 5 represent the intensity dependence for different effective background illuminations  $I_\beta = 0.0036 \text{ W/cm}^2$ ,  $I_\beta = 0.018 \text{ W/cm}^2$  and  $I_\beta = 0.072 \text{ W/cm}^2$ . The solid curve in Fig. 5 represents a calculation including the correction factor  $\xi$  for the intensity ratio for a background illumination of  $I_\beta = 0.0144 \text{ W/cm}^2$ , which is of the same order of magnitude as observed for yellow and brown crystals at 633 nm for a ring-cavity self-pumped phase conjugate mirror [22].

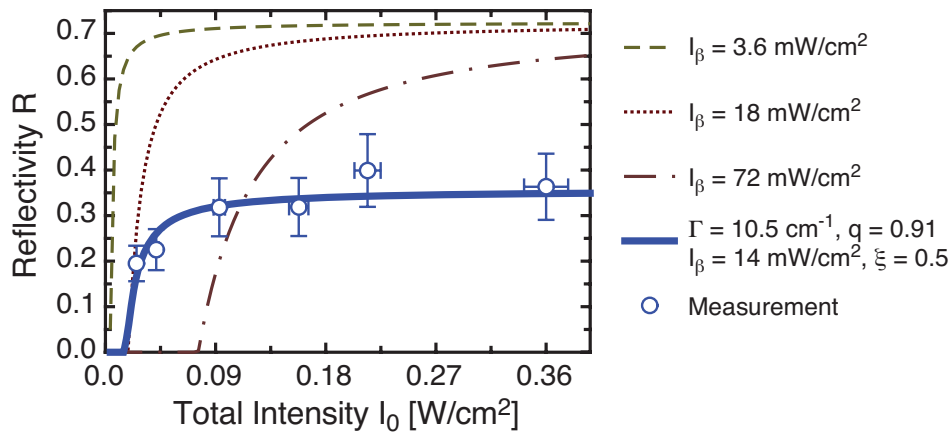


Fig. 5. Saturated phase conjugate reflectivity  $R$  as a function of the total intensity  $I_0$ . Dotted/dashed curves represent calculations based on Eq. (1) considering the background illumination  $I_\beta$  leading to a modified parameter  $\kappa$  according to Eq. (7). The solid curve additionally considers the absorption loss in the crystal in the correction parameter  $\xi$ , as described by Eq. (6).

### 3.2. Double phase conjugation of multiple beams and locking of one emitter

For coupling the laser diode bar with a single mode laser diode we used pure  $\text{Sn}_2\text{P}_2\text{S}_6$  in the double phase conjugate mirror. The experimental set-up is illustrated in Fig. 2 and described in the experimental part.

In the first experiment we used only one emitter of the laser diode bar. At a driving current of 4 A, the power of each emitter was  $\approx 50$  mW. The single-mode master laser was operating with 30 mW at a wavelength of  $(684.1 \pm 0.1)$  nm. For the yellow  $\text{Sn}_2\text{P}_2\text{S}_6$  crystal the angles of incidence for the beams to the crystal were  $\theta_1 = 25^\circ$  and  $\theta_2 = 50^\circ$ . The difference angle  $\theta_2 - \theta_1 = 25^\circ$  corresponds to the highest measured two-wave mixing gain  $\Gamma$  at the grating spacing  $\Lambda = 1.5 \mu\text{m}$  [26]. For this configuration we could observe the locking of the laser diode bar to the single-mode master laser. This means that the phase conjugated beam of the slave laser beam from the laser diode bar was redirected into the active area of the diode bar. This phase conjugated beam had the spectral properties of the single-mode master laser. In the active area of the laser diode bar the mode of the phase conjugated beam was amplified and the other modes were suppressed. A comparison between the spectrum of a free running and a locked emitter of the laser diode bar can be seen in Fig. 6. For measurement of the spectra a photo-spectrometer (Andus) was used. The free running emitter of the laser diode oscillated at a center wavelength of  $(684.2 \pm 0.1)$  nm with a spectral width of  $\Delta\lambda \approx 0.5$  nm. After locking, the center wavelength was at  $(684.1 \pm 0.1)$  nm, just like the single-mode master laser, as expected. From the measurement with the spectrometer we obtained a spectral width of  $\Delta\lambda \approx 0.073$  nm, which presents the resolution limit of our spectrometer. Measurements with a Fabry-Perot interferometer led to a spectral width for the locked emitter of the laser diode bar of  $\Delta\lambda < 2.5 \cdot 10^{-4}$  nm.

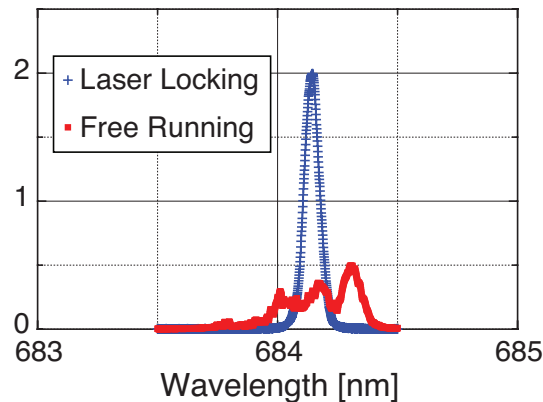


Fig. 6. Comparison of the free running mode and the locked mode spectrum of the slave laser output measured with a spectrometer. One diode of the laser bar is coupled with the master laser ( $I_M = 0.20 \text{ W/cm}^2$ ) and the intensity of the slave laser beam before entering the crystal is  $I_S = 0.36 \text{ W/cm}^2$ .

In a next step we obtained phase conjugation of more than one emitter of the laser diode bar. Different emitters work independently from each other, therefore one can consider this experiment as phase conjugation of a master laser with several independent slave laser sources. We performed the experiment with three emitters having the center wavelength between 683.5 nm and 684.5 nm. Figure 7 shows the phase conjugated image of the three emitters seen on a white screen. Double phase conjugation of three independent laser sources with a master laser was possible. If more than three emitters of the laser diode bar were used, the phase conjugated

beams (image) became weaker and was finally erased. Additional beams from emitters of the laser diode bar did not build up new gratings with the master laser; on the contrary, they erased the gratings previously recorded in the crystal.

The process of double phase conjugation with three emitters was independent of the wavelength of the master laser within its tuning range of  $\sim 683\text{--}686\text{ nm}$ . Therefore double phase conjugation with three emitters of the laser diode bar was always possible using the particular set-up. However, for locking an emitter of the slave laser, the center wavelengths of the master and the slave laser had to be the same within a range of  $\sim 0.1\text{ nm}$ . Having a higher difference of the wavelengths of the master laser and the (unlocked) slave lasers, the phase conjugated beam was redirected back slightly off the original direction. The phase conjugated beam, which was supposed to lock the laser diode, failed the aperture of the active area of the laser diode. Therefore it was possible to lock each of the emitters of the laser diode bar by adjusting the wavelength of the master laser. The spectral properties were the same as in the previous experiment (double phase conjugation with one emitter of the laser diode bar, Fig. 6).



Fig. 7. Double phase conjugated image observed on the screen of three independent emitters of a laser diode bar.

#### 4. Conclusion

We demonstrated for the first time to the very best of our knowledge simultaneous double phase conjugation in the photorefractive ferroelectric material  $\text{Sn}_2\text{P}_2\text{S}_6$  (in nominally pure and in Te-doped  $\text{Sn}_2\text{P}_2\text{S}_6$ ) at the wavelength 685 nm. Double phase conjugate reflectivity of more than 800 percent was measured for an intensity ratio of the input pump beams of  $q \approx 44$ . The measurement of the variation of the input beam ratio  $q$ , as well as the variation of the total intensity could be well explained by a modified model of the coupled-wave theory.

Using a laser diode bar at 685 nm we demonstrated double phase conjugation of three independent laser sources (emitters of the laser diode bar) with a single mode master laser. By adjusting the center wavelength of the master laser to the center wavelength of an emitter with an accuracy of less than 0.1 nm, locking of any emitter of the laser diode bar was possible. We improved the spectral width for the emitter from 0.5 nm to below  $2.5 \cdot 10^{-4}\text{ nm}$ .

#### Acknowledgments

We thank A. A. Grabar and Y. M. Vysochanskii for supplying the crystals, J. Hajfler for polishing the crystals and the Swiss National Foundation for the financial support.